



Structure-based 3D QSAR and design of novel acetylcholinesterase inhibitors

Wolfgang Sippl^{a,*}, Jean-Marie Contreras^b, Isabelle Parrot^b, Yveline M. Rival^b & Camille G. Wermuth^b

^a*Institut für Pharmazeutische Chemie, Heinrich-Heine-Universität Düsseldorf, Universitätsstr. 1, D-40225 Düsseldorf, Germany;* ^b*Laboratoire de Pharmacochimie de la Communication Cellulaire, UMR 7081 du CNRS, Université Louis Pasteur, Faculté de Pharmacie, 74, route du Rhin, 67401 Illkirch Cedex, France*

Received 3 October 2000; accepted 4 January 2001

Key words: acetylcholinesterase inhibitors, CoMFA, Docking, GOLPE, GRID, 3D QSAR, structure-based design

Summary

The paper describes the construction, validation and application of a structure-based 3D QSAR model of novel acetylcholinesterase (AChE) inhibitors. Initial use was made of four X-ray structures of AChE complexed with small, non-specific inhibitors to create a model of the binding of recently developed aminopyridazine derivatives. Combined automated and manual docking methods were applied to dock the co-crystallized inhibitors into the binding pocket. Validation of the modelling process was achieved by comparing the predicted enzyme-bound conformation with the known conformation in the X-ray structure. The successful prediction of the binding conformation of the known inhibitors gave confidence that we could use our model to evaluate the binding conformation of the aminopyridazine compounds. The alignment of 42 aminopyridazine compounds derived by the docking procedure was taken as the basis for a 3D QSAR analysis applying the GRID/GOLPE method. A model of high quality was obtained using the GRID water probe, as confirmed by the cross-validation method ($q_{\text{LOO}}^2 = 0.937$, $q_{\text{L50\%O}}^2 = 0.910$). The validated model, together with the information obtained from the calculated AChE-inhibitor complexes, were considered for the design of novel compounds. Seven designed inhibitors which were synthesized and tested were shown to be highly active. After performing our modelling study the X-ray structure of AChE complexed with donepezil, an inhibitor structurally related to the developed aminopyridazines, has been made available. The good agreement found between the predicted binding conformation of the aminopyridazines and the one observed for donepezil in the crystal structure further supports our developed model.

Introduction

The neurodegenerative Alzheimer's disease (AD) affecting mainly aging populations in industrialised nations is characterised by three major pathological signs: β -amyloid plaques, neurofibrillary tangles, and synaptic loss [1, 2]. A deficiency in cholinergic neurotransmission is considered to be one of the major causes of memory impairments in patient [3, 4]. A palliative treatment of AD is possible by the use of agents which restore the level of acetylcholine [5]. Acetyl-

cholinesterase (AChE) inhibitors such as tacrine [6], donepezil [7], galanthamine [8] and rivastigmine [9] are able to enhance memory in AD patients. Recent studies [10, 11] have shown that AChE inhibitors, especially mixed-type inhibitors, which interact with the peripheral site of the enzyme, could, in addition to AChE inhibition, act as potential inhibitors of the formation of β A4-amyloid protein [12, 13]. Thus, centrally active AChE inhibitors represent a promising approach to the treatment of AD. In this context we focused on the search for novel potent and selective AChE inhibitors that interact with the peripheral site of the enzyme. In a recent paper [14], we reported the

*To whom correspondence should be addressed: E-mail: sippl@pharm.uni-duesseldorf.de

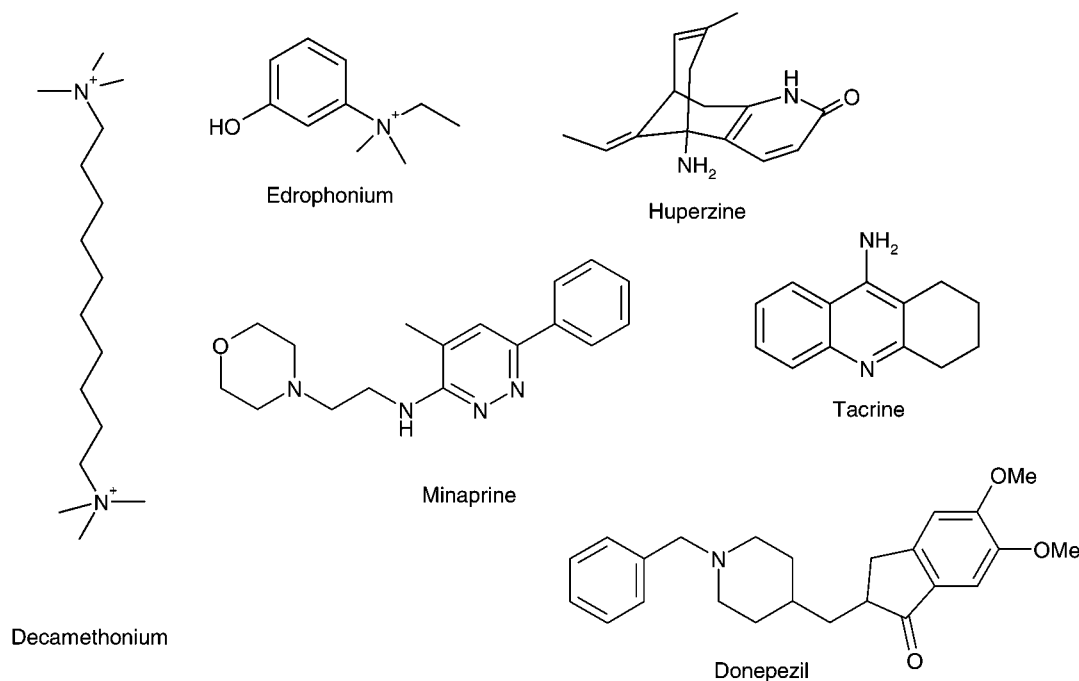


Figure 1. Molecular structures of AChE inhibitors.

synthesis and the biochemical evaluation of a series of 3-aminoalkyl-6-arylpyridazine derivatives based on the structure of minaprine (Figure 1), an original lead compound with antidepressive properties [15]. As a complement, we would like to report here the underlying molecular modelling work which was initiated in order to design novel AChE inhibitors.

The availability of several crystal structures of AChE [16–18] in complex with the inhibitors tacrine, edrophonium, huperzine A, and decamethonium provides the possibility to apply structure-based drug design techniques to the development of specific and potent inhibitors for this enzyme. Using the data derived from the crystal structure of AChE, along with a docking protocol, low-energy conformations for the protein-inhibitor complex are generated. One major problem of today's docking protocols is the inability to evaluate binding free energies correctly in order to rank different protein-ligand complexes. Since docking programs generate a huge amount of possible protein-ligand complexes, it is difficult to determine *a priori* which ligand conformation represents the bioactive one. The problem of predicting affinity has generated considerable interest in developing new methods to calculate ligand affinity reliably for a widely diverse series of molecules [19–23]. Until now only rigorous methods, such as the free energy pertur-

bation methods, are able to correctly predict binding affinity. Since these methods are computationally very intensive, they cannot be applied to large ligand series, commonly studied in QSAR analysis.

Very recently several studies have been published in which the combination of receptor-based methods and 3D QSAR was successfully applied for the design and prediction of bioactive compounds [24–28]. The three-dimensional structure of a target protein, along with a docking protocol is used to guide alignment selection for comparative molecular field analysis. It is quite appealing to combine the accuracy of a receptor-based alignment with the computational efficiency of a ligand-based method. Receptor structures, either experimentally resolved or obtained by homology modelling, can provide important information that is critical for an alignment in CoMFA, while QSAR can provide better prediction of binding energies [28].

In the present study we use the combination of receptor-based alignments and 3D QSAR methods to calculate the biological activities of a set of 42 AChE inhibitors [14]. On the basis of the developed 3D QSAR model, novel molecules are designed and their activities are predicted.

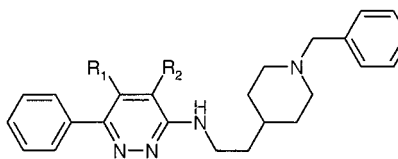
Table 1. Structures and activities of studied compounds (1)

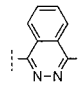
$$\text{Ph}-\text{C}_4\text{H}_3\text{N}_2-\text{NH}_2-(\text{CH}_2)_n-\text{R}$$

Compnd.	<i>n</i>	<i>R</i>	pIC ₅₀ ^a	Predicted pIC ₅₀ ^b
3a	2		3.10	3.04
3m	3		3.39	3.55
3b	2		4.19	4.12
3o	2		4.08	3.98
3p	3		4.46	4.38
3q	4		4.82	4.79
3r	5		5.00	4.93
3s	2		3.77	3.86
3t	3		4.89	4.76
3u	4		4.96	4.97
3v	5		6.13	6.12
3w	0		4.19	4.17
3x	1		5.25	5.23
3y	2		6.92	6.93
Minaprine ^c			3.21	3.31

^aInhibitory activity measured on the AChE of *Torpedo californica* [14, 29]^bPredicted activity using the LOO cross-validated water probe model (4 principal components).^cSee Figure 1.

Table 2. Structures and activities of studied compounds (2)



Compnd.	R ₁	R ₂	pIC ₅₀ ^a	Predicted pIC ₅₀ ^b
4a	H	Me	6.49	6.41
4b	H	i-Pr	6.37	6.35
4c	Me	H	7.68	7.41
4d	Et	H	7.57	7.61
4e	Pr	H	7.21	7.57
4f			6.36	6.51

^aInhibitory activity measured on the AChE of *Torpedo californica* [14, 29].^bPredicted activity using the LOO cross-validated water probe model (4 principal components).

Methods

Data set

For the investigation structure-activity data for a series of 42 AChE inhibitors were considered. The synthesis and the biological testing is reported [14, 29]. The molecular structures of these 42 inhibitors are represented in Tables 1–5. Inhibitory activity was measured on electric eel AChE by the spectrophotometric method of Ellman et al. [30]. These numbers were then transformed to decadic log values which were used in the present 3D QSAR analysis.

Building the inhibitors

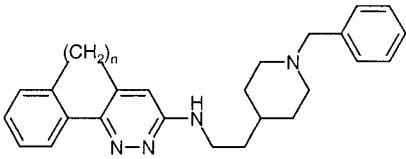
The molecular modelling studies were performed on a Silicon Graphics Indigo2 R10000 using the SYBYL 6.5 software package from Tripos, Inc St. Louis, MO. The crystal structure of minaprine (Figure 1) retrieved from the Cambridge Structural Database [31], was used as template to construct the inhibitors. All molecules were assumed to be mono-protonated under physiological conditions and their molecular struc-

tures were accordingly generated. AM1-ESP [32] charges were calculated for the inhibitors.

Crystal structures

The crystal structures of AChE from *Torpedo californica* complexed with decamethonium, edrophonium, huperzine A and tacrine (Figure 1) were retrieved from the Brookhaven Protein Database [16–18] (1ACL liganded with decamethonium, 2ACK liganded with edrophonium, 1ACJ liganded with tacrine and 1VOT liganded with huperzine A). Polar hydrogen atoms were added using the BIOPOLYMER module within SYBYL and charges from AMBER [33, 34] were loaded. The ionization states of the protein residues were determined from pKa calculations using the UHBD program [35]. Specifically, charges of the catalytic triad were as follows: His447 was neutral, with the position of the hydrogen at the epsilon nitrogen, Glu202 was unprotonated with a –1 charge, and Ser was considered neutral. All water molecules observed in the crystal structure were deleted. The whole molecule was subjected to a minimization using the AMBER4.1 force field [33, 34] (as implemented in SYBYL6.5) keeping all protein back-bone atoms at

Table 3. Structures and activities of studied compounds (3)



Compnd.	<i>n</i>	pIC ₅₀ ^a	Predicted pIC ₅₀ ^b
4j	3	7.66	7.53

^aInhibitory activity measured on the AChE of *Torpedo californica* [14, 29].

^bPredicted activity using the LOO cross-validated water probe model (4 PC).

fixed positions. Energy minimization was carried out for 500 steps with the steepest descent minimizer and subsequently for 2000 steps with the conjugate gradient minimizer. These energy-minimized structures were used for docking studies.

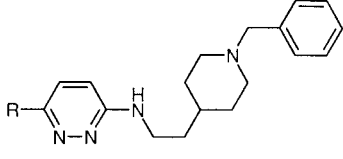
Molecular interaction fields

To investigate the interaction potentials of the protein and inhibitor structures, we performed a series of GRID [36] calculations. Program GRID is an approach to predict noncovalent interactions between a molecule of known three-dimensional structure (i.e. the AChE protein) and a small group as a probe (representing chemical features of a ligand). The calculations were performed using version 16 of the GRID program and the crystal structures mentioned above. The calculations were performed on a cube ($21 \times 25 \times 28$ Å, spacing 1 Å) including the binding pocket in order to search for binding sites complementary to the functional groups of the inhibitors. Several probes were used to study the active site of the AChE (carbonyl, trimethylammonium and hydrophobic DRY probe). The calculated GRID contour maps were then viewed superimposed on the crystal structure of the AChE using the SYBYL 6.5 software.

Docking protocol

For the current work, we use a combination of automated and manual docking. The automated docking analysis was performed using the program AutoDock (version 2.4), which has been shown to successfully reproduce experimentally observed binding modes [37–39]. (The program is described in detail elsewhere [37]). In a second step, the inhibitor conformations

Table 4. Structures and activities of studied compounds (4)



Compnd.	<i>R</i>	pIC ₅₀ ^a	Predicted pIC ₅₀ ^b
4k	H	6.62	6.78
5	Cl	7.14	7.02
7	MeO	6.66	6.97
6a	2-Me-Ph	7.05	6.99
6b	2-Et-Ph	7.06	7.03
6c	2,4,6-(Me) ₃ -Ph	5.53	5.69
6d	2-MeO-Ph	6.96	6.90
6e	2-Cl-Ph	7.10	6.99
6f	3,5-(CF ₃) ₂ -Ph	7.25	7.24
6k	2-thiophenyl	7.01	6.91
6l	3-pyridinyl	7.24	7.17

^aInhibitory activity measured on the AChE of *Torpedo californica* [14, 29].

^bPredicted activity using the LOO cross-validated water probe model (4 PC).

which showed the best agreement with the GRID interaction fields (calculated for the free binding pocket) were manually selected. AutoDock considers only the polar hydrogen atoms during the docking process, and uses simple potential functions for the calculation of the binding energy. Therefore, the obtained protein-ligand complexes were further refined in a second step applying a more sophisticated optimization procedure. All hydrogen atoms were added to the protein structure and the resulting complexes were minimized using the YETI force field [40, 41]. This force field has been validated on protein-ligand complexes and was therefore well suited for the present task [42]. A region of 8 Å around any inhibitor atom was defined flexible during this optimization step. The protein-ligand interaction energies were then calculated using the refined complexes.

3D QSAR analysis

The GRID/GOLPE method was used within this study to perform a 3D QSAR analysis [43, 44]. The interaction field between the ligands and (a) the water and (b) the methyl probe was calculated by applying the GRID program employing a grid spacing of 1 Å. The size of the grid box considered for the calculation was defined in such a way that it extended approximately

Table 5. Structures and activities of studied compounds (5)

Compnd.	X	Y	pIC ₅₀ ^a	Predicted pIC ₅₀ ^b
10	OCH ₂ CH ₂		6.85	6.92
12	SCH ₂ CH ₂		7.20	7.16
14a	NHCOCH ₂		5.38	5.27
16a	NHCH ₂ CH ₂		5.82	5.40
14b	NHCOCH ₂		4.77	4.75
18a	NHCH ₂ CO		4.82	4.64
16b	NHCH ₂ CH ₂		4.62	5.22
14c	NHCOCH ₂		4.74	4.79
18b	NHCH ₂ CO		3.92	4.10

^aInhibitory activity measured on the AChE of *Torpedo californica* [14, 29].^bPredicted activity using the LOO cross-validated water probe model (4 PC).

4 Å beyond each of the molecules in each dimension (21 × 25 × 28 Å). A cutoff of +5 kcal/mol was applied in order to obtain a more symmetric distribution of energy values. The GRID calculation gave 17160 variables for each compound. A major part of these variables is not important for describing the interaction between the ligand and the receptor and is introducing only noise in the statistical PLS analysis [45]. These variables were selected and eliminated applying the advanced pretreatment procedure and the SRD/FFD (Smart Region Definition/Fractional Factorial Design) variable selection within the GOLPE program (for a detailed description of this approach, see [44–46]). Models obtained applying variable selection are in general of higher quality than models calculated without variable selection. The GOLPE advanced pretreatment eliminated those variables with absolute values smaller than 0.05 kcal/mol and variables with a standard deviation below 0.02 kcal/mol. In addition, variables which take only two or three values were also removed. After this pretreatment the data set still contains 5464 variables for the water and

4456 variables for the methyl probe. Subsequently, the SRD procedure was used to carry out the variable selection on groups of variables chosen according to their positions in 3D space [46]. Within the SRD procedure 500 seeds, a critical distance cutoff of 1.0 Å and a collapsing distance cutoff of 2.0 Å were applied. The regions calculated were then used in a FFD variable selection procedure. The number of variables was reduced to 576 for the water and to 1097 for the methyl probe with major improvement of the quality of the model.

Model validation

To form the basis for a statistical significant model, the method of partial least squares (PLS) regression was used to analyze the 42 compounds by correlating variations in their biological activities with variations in their interaction fields. The optimum number of PLS components corresponding to the smallest standard error of prediction, was determined by the leave-one-out (LOO) cross-validation procedure. Using the optimal number of components, the final PLS analysis

was carried out without cross-validation to generate a predictive model with a conventional correlation coefficient. The LOO cross-validation method might lead to high q^2 values which do not necessarily reflect a general predictiveness of a model. Therefore a second cross-validation, selecting two groups of approximately the same size in which the objects were assigned randomly, was performed. In this method, 50% of the compounds were randomly selected and a model is generated, which is then used to predict the remaining compounds (leave-50% -out, L50%O). This cross-validation technique has been shown to yield better indices for the robustness of a model than the normal LOO procedure [47].

To further evaluate the predictive ability of the resulting model, a test set of seven designed molecules was utilized (Table 7). The alignment of these compounds was generated applying the described AutoDock/Yeti procedure. Their activities were predicted choosing the best GRID/GOLPE model.

Results and Discussion

Binding orientation of AChE inhibitors

The detailed inspection of the four AChE-inhibitor X-ray structures yielded crucial information concerning the orientation of the inhibitors in the binding pocket. Knowledge of the ability of a protein to alter its conformation to accommodate a binding ligand, is crucial to the process of predicting new inhibitors. Access to the crystal structures of AChE complexed separately with the four inhibitors tacrine, decamethonium, huperzine A and edrophonium enabled us to directly compare the relative positions of the residues in the binding pocket. AChE shows a nearly identical three-dimensional structure in all known X-ray structures. The active site is located 20 Å from the protein surface at the bottom of a deep and narrow gorge. The only major conformational difference between the four complexes is the orientation of the phenyl ring of Phe330, a residue located in the middle of the gorge (Figure 2). Depending on the co-crystallized inhibitor, this aromatic residue adopts a different conformation. However the position of the four inhibitors in the binding pocket is quite different, indicating that more than one clearly defined binding region exists. The known crystal structures of AChE-inhibitor complexes were taken as positive controls for the performance of our docking approach.

Applying program GRID we inspected the interaction possibilities at the binding pocket. The calculated GRID contour maps, obtained with a variety of probes, were then viewed superimposed on the crystal structure of the AChE. We observed a good agreement of the location and size of the GRID fields with the corresponding functional groups of the co-crystallized inhibitors. As examples, the results obtained with the carbonyl and the trimethylammonium probe are shown in Figure 3. GRID detected a favorable interaction field for the trimethylammonium probe 4 Å above the indole ring of Trp84. It agrees perfectly with the position found for the quaternary group of decamethonium and edrophonium in the corresponding X-ray structure (Figure 3a). Taking the derived interaction fields as filters along with the complexes generated by the AutoDock/YETI procedure, we were able to select the co-crystallized conformation of all four inhibitors. A good agreement was only observed when the AChE crystal structure extracted from the corresponding protein-inhibitor complex was taken as target for the docking simulation. The RMSD values (heavy atoms) between theoretically predicted and experimentally determined positions are for tacrine: 0.28 Å; for huperzine A: 0.51 Å; for edrophonium: 0.71 Å and for decamethonium: 1.15 Å.

Docking of aminopyridazine compounds

The ability to accurately predict the binding conformations of tacrine, decamethonium, edrophonium and huperzine A gave confidence that we could use our model to evaluate the binding conformations of the aminopyridazine compounds. We selected all four available AChE structures as target for the docking of the aminopyridazine derivatives. Only in case of the AChE structure retrieved from the AChE-decamethonium complex AutoDock was able to find low energy complexes where the inhibitors interact with the active site. That means only when the side-chain of Phe330 is orientated perpendicular to the gorge (as in the AChE-decamethonium complex) the larger aminopyridazine inhibitors are able to interact with residues at the bottom of the binding pocket.

The results of the docking studies allowed us the identification of key features of the aminopyridazine inhibitors that are responsible for their high potency. As an example, the key interactions of compound **3y** are shown in Figure 4. The positively charged piperidine nitrogen makes a cation- π interaction with Phe330 and Trp84 and electrostatic interactions with

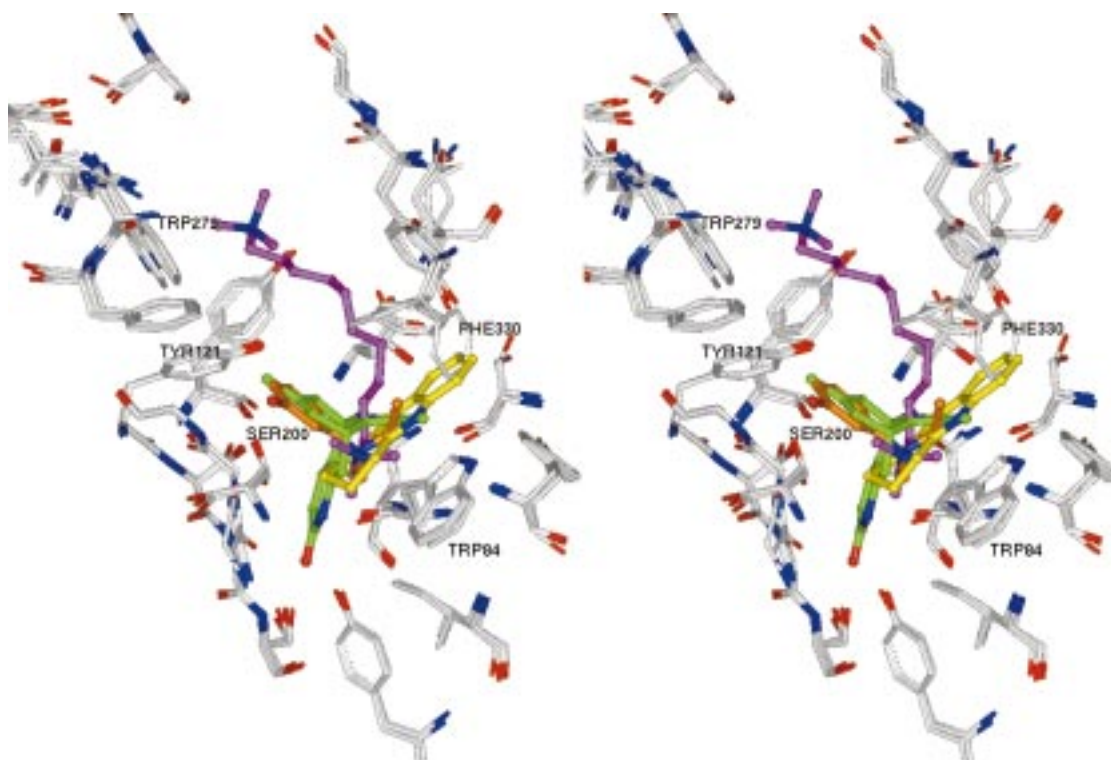


Figure 2. Stereo view of the superimposed crystal structures of AChE liganded with huperzine A (green), tacrine (yellow), edrophonium (orange) and decamethonium (magenta). Only the amino acid residues close to the binding site are displayed. The only major conformational difference between the four complexes is the orientation of the phenyl ring of Phe330, a residue located in the middle of the gorge.

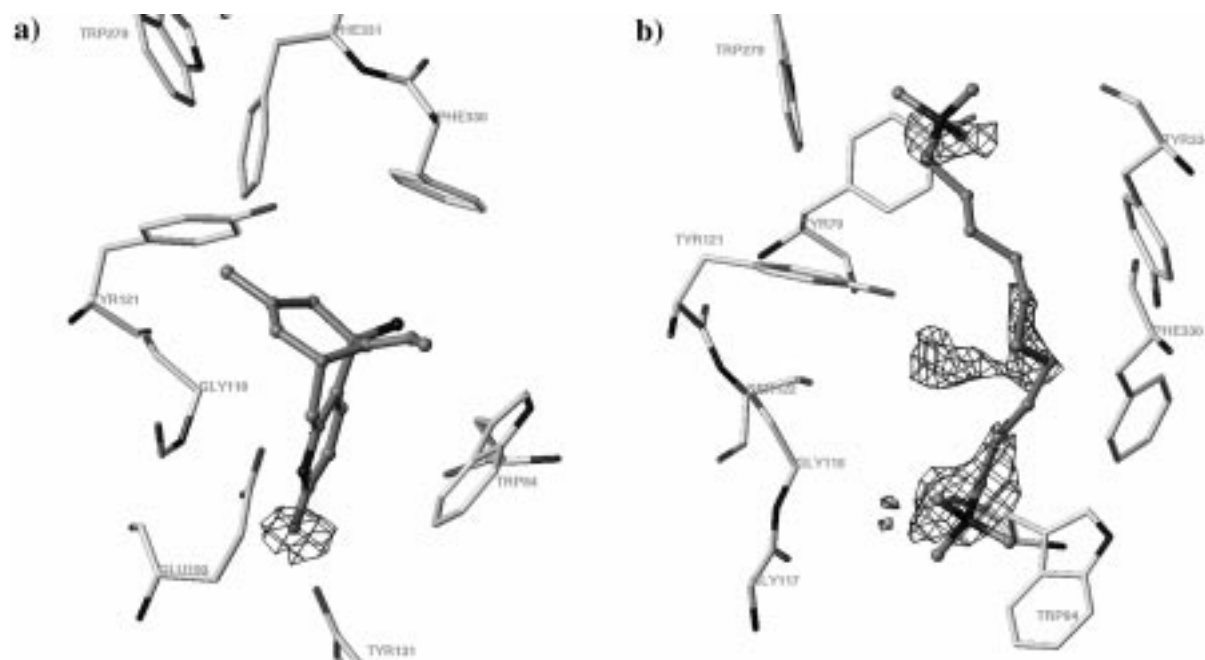


Figure 3. GRID interaction fields calculated for the uncomplexed AChE: a) Favorable regions of interaction between the carbonyl probe and the active site (contoured at an energy level of -5 kcal/mol). Huperzine A is displayed for comparison. b) Favorable regions of interaction between the trimethylammonium probe and the active site (contoured at an energy level of -9.5 kcal/mol). Decamethonium is displayed for comparison.

Table 6. Statistical results of the GRID/GOLPE PLS models

GRID probe	r^2	SDEC	q^2_{LOO}	SDEP	$q^2_{\text{L50\%O}}$	SDEP	SDEP _{ext}
Water ^a	0.990	0.141	0.937	0.345	0.910	0.409	0.440
Methyl ^b	0.981	0.186	0.923	0.377	0.895	0.440	0.398

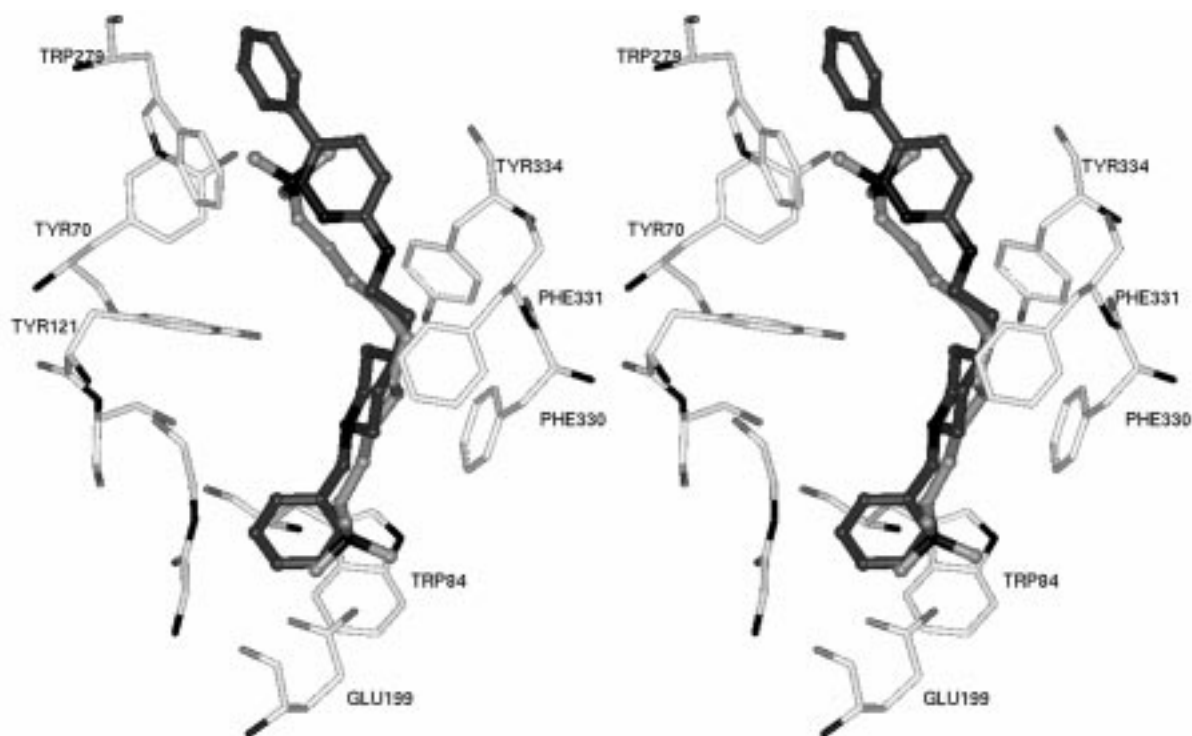
^aFour principal components.^bThree principal components.

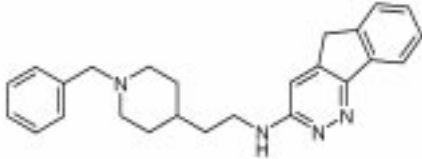
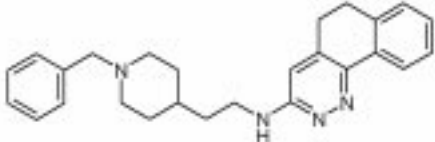
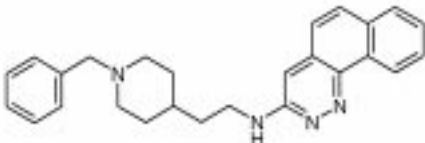
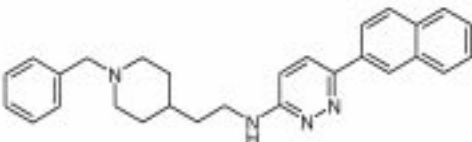
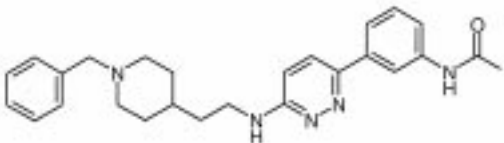
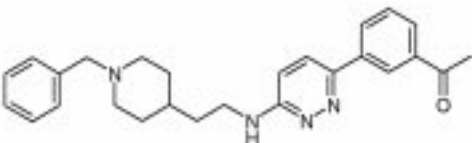
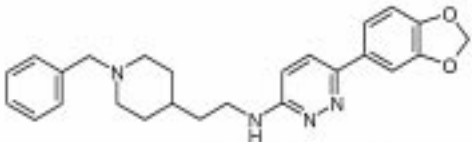
Figure 4. Stereo view of the predicted position of compound **3y** (dark-gray) and the X-ray structure of decamethonium (gray). Only the amino acid residues of the binding pocket are displayed for clarity.

Tyr121 and Ser122. The distance between the charged nitrogen atom and the aromatic rings systems of Trp84 and Phe330 lies in the range between 4.0 Å and 4.5 Å.

Hydrophobic and Van-der-Waals interactions are also evident for the protein-inhibitor model. The gorge leading to the active site is lined with aromatic residues, which constitute ca. 40% of the residues present in the binding pocket. Our inhibitors take advantage of this aromatic residues by making a variety of interactions. Van-der-Waals interactions of the piperidine ring occur with Phe331 and Tyr334. The benzyl ring of the inhibitor displays π - π stacking with the aromatic ring of Trp84. It occupies the binding site for the quaternary ligands, such as edrophonium or decamethonium. The aminopyridazine part of the inhibitors is located at the entrance of

the gorge and interacts with two aromatic residues (Trp279 and Tyr70). Thus, the aminopyridazine ring occupies the same region in space as the quaternary trimethylammonium group of decamethonium in the corresponding X-ray structure. The hydrophobic interaction possibilities of the inhibitors have been analyzed using the GRID interaction field obtained with the hydrophobic DRY probe (Figure 5). The calculated field is superimposed on the structure of the active site. There exist two main regions in the binding pocket where program GRID has detected favorable hydrophobic interactions. Both regions can be occupied by the aliphatic or aromatic fragments of the aminopyridazine inhibitors. Inhibitors containing bulky groups attached to the aminopyridazine show

Table 7. Structures and activities of seven designed ACLE inhibitors

Compnd.	Structure	Observed ^a	Predicted ^b	Predicted ^c
4g		8.00	7.00	7.20
4h		7.41	7.62	7.66
4i		7.66	7.48	7.56
6g		7.24	6.90	6.77
6h		7.24	7.05	7.11
6i		7.27	7.25	7.2
6j		7.14	6.88	6.92

^aInhibitory activity measured on the AChE of *Torpedo californica* [14].^bPredicted activity using the water probe model (4 principal components).^cPredicted activity using the methyl probe model (3 principal components).

the highest potency among the series, pointing out the influence of the hydrophobic interaction in this area.

Surprisingly, we observed no direct hydrogen bond between the polar groups of the inhibitors and the

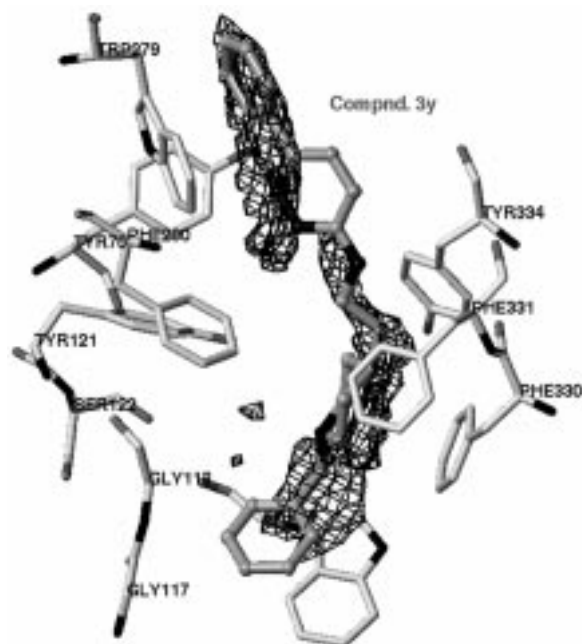


Figure 5. Favorable regions of interaction between the hydrophobic DRY probe and the active site (contoured at an energy level of -0.6 kcal/mol). Compound **3y** is displayed for comparison.

binding site. However, the polar atoms of the inhibitors are located in the proximity of polar amino acid residues. Thus, it is possible that water molecules bridge the distance between inhibitor and the protein. Water-bridged hydrogen bonds may occur between the piperidine nitrogen of the inhibitors and Tyr121 or Ser122. An additional water-bridged hydrogen bond may occur between the backbone atoms of Phe288 and the amino-group of the aminopyridazine structure. Comparable water-bridged hydrogen bonds has been observed in the X-ray structures of the AChE complexed with huperzine A, decamethonium or tacrine.

In the next step, we calculated the protein-inhibitor interaction energies (using the TRIPOS and the YETI force field) and correlated them with the biological activities. Only low to moderate correlation coefficients were obtained depending on the chosen protocol (data not shown). For this reason, we took the superimposition of the ligands derived from the molecular docking for a comparative molecular field analysis using the strategy described in the methods section.

Receptor-based 3D QSAR model

The alignment of all inhibitors is displayed together with the molecular surface of the binding pocket in

Figure 6. The LOO cross-validated q_{LOO}^2 values for the initial models was 0.875 using the water probe (four components) and 0.850 using the methyl probe (three components). The application of the SRD/FFD variable selection resulted in an improvement of the significance of both models. The analysis yielded a correlation coefficient with a cross-validated q_{LOO}^2 of 0.937 for the water probe and 0.923 for the methyl probe (Figure 7, only the correlation for the water probe is shown). The conventional r^2 values of these analyses are 0.990 (water probe) and 0.981 (methyl probe). This means, that both models explain approximately more than 98% of the variance in ligand binding of the investigated compounds. Both models are also robust, indicated by high correlation coefficients of $q^2 = 0.910$ (water probe) and 0.895 (methyl probe) obtained by using the leave-50% -out cross-validation procedure (the statistical results are summarized in Table 6).

Design of novel inhibitors

To get an impression which parts of our inhibitors are correlated with variation in activity we analyzed the PLS coefficient plots (obtained using the water and the methyl probe) and compared them with the amino acid residues of the binding pocket. The plots indicate those lattice points where a particular property significantly contributes and thus explains the variation in biological activity data. The coefficient plots for the water and methyl probes used in the GRID calculations are almost identical indicating that the differences in activity between the inhibitors is mainly due to steric interactions with the target (Figure 8). The plot obtained with the methyl probe indicates that close to the arylpyridazine part, a region with positive coefficients exists (region A in Figure 8). The coefficients were superimposed with the original GRID field obtained for compound **4j** with the methyl probe. The interaction energies in region A are positive, therefore the decrease in activity is due to overlapping of this region. Thus, it should be possible to get active inhibitors by reducing the ring size compared to compound **4j** (which is shown in Figure 8 together with the PLS coefficient maps). For that reason, several molecules containing hydrophobic groups were proposed (Table 7, compounds **4g–4i** and **6g**). A second interesting field was observed above the arylpyridazine moiety in the model obtained using the water probe. There exists a region where polar interaction increase activity (region B in Fig-

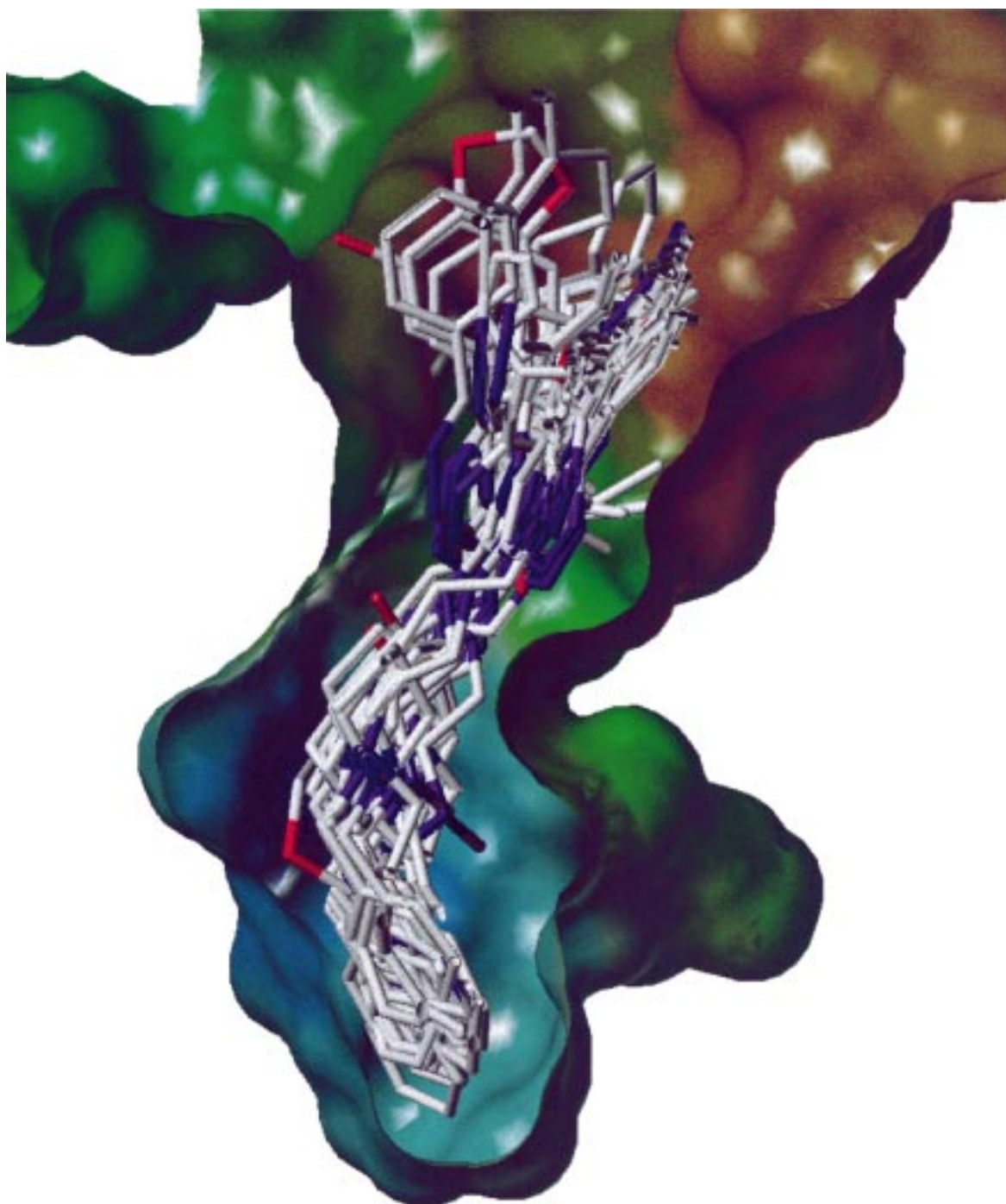


Figure 6. The figure shows the superposition of all investigated inhibitors as obtained by the docking experiment. The protein surface is colored according to the hydrophobic potential (blue = hydrophilic areas, brown = hydrophobic areas, calculated with the MOLCAD software).

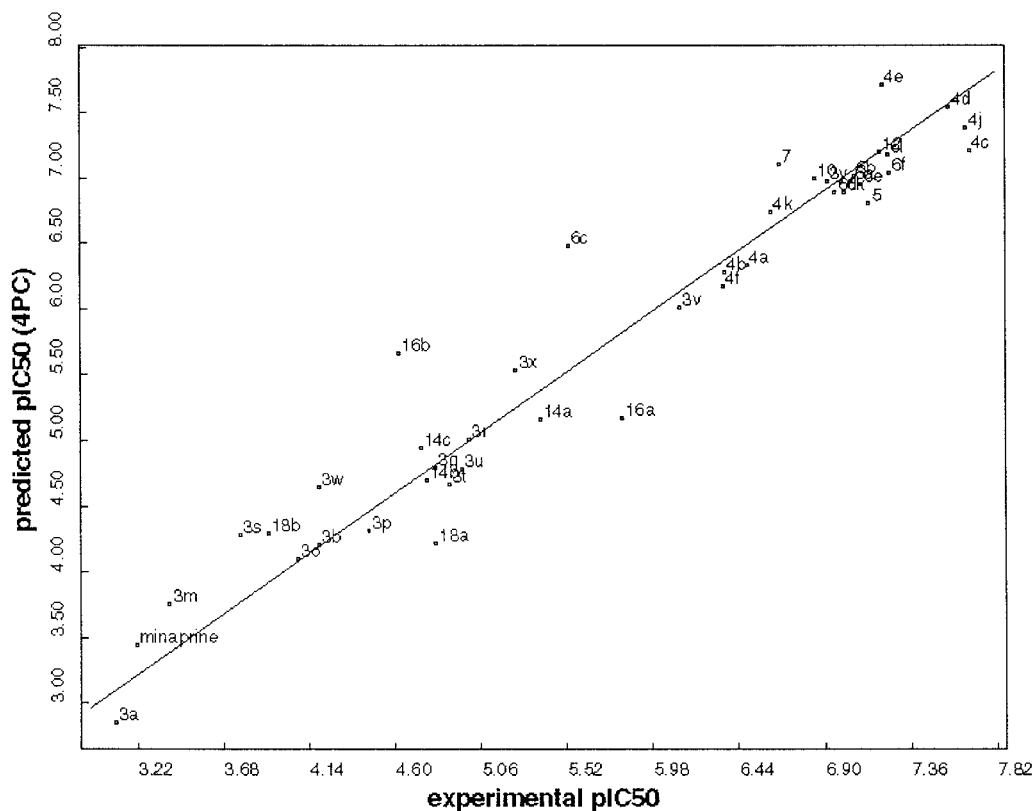


Figure 7. The figure shows the predicted vs. experimental activity for the resulting GRID/GOLPE model (four principal components) obtained using the water probe.

ure 8). Together with an analysis of the entrance of the gorge, the interaction site for the arylpyridazine system, we got the idea to design compounds containing polar groups in that region. In the calculated AChE-aminopyridazine complexes we observed two polar amino acid residues (Asn280 and Asp285) located at the entrance of the gorge which could serve as additional binding sites for the substituted arylpyridazine system. To test this hypothesis, several inhibitors possessing functional groups with hydrogen bond donor and acceptor properties were synthesized and tested (Table 7, compounds **6h–6j**). The designed inhibitors were docked in the binding pocket applying the developed procedure and their biological activities were predicted using the GRID/GOLPE PLS models. The seven compounds were considered as external test set. Table 7 shows the predicted and experimentally determined inhibitor activities for these compounds. In general a good agreement between predicted and experimentally determined values was observed, indicated by the low $SDEP_{ext}$ values of 0.440 (water model) and 0.398 (methyl model). The reducing of

the size of the aminopyridazine ring system resulted in highly potent inhibitors **4g–4i**. However, compound **4g** shows the largest difference between predicted and actual. The molecules of the second series of designed inhibitors containing polar groups were also accurately predicted. The gain in activity compared to the nonsubstituted compound **3y** is moderate, indicating that the potential interaction with the two polar residues at the entrance does not play an important role. Since the two residues are located at the entrance of the binding pocket, it may be possible that these residues make stronger interaction to water molecules. This fact is further supported by the X-ray structures of the AChE-inhibitor complexes where the entrance of the binding pocket is filled with many water molecules.

In conclusion, we were able to design AChE inhibitors based on our molecular docking study which seems to interact simultaneously with the cation- π sub-site of the catalytic site and the peripheral site of the enzyme. After we had performed our modelling studies, experimental data have been published

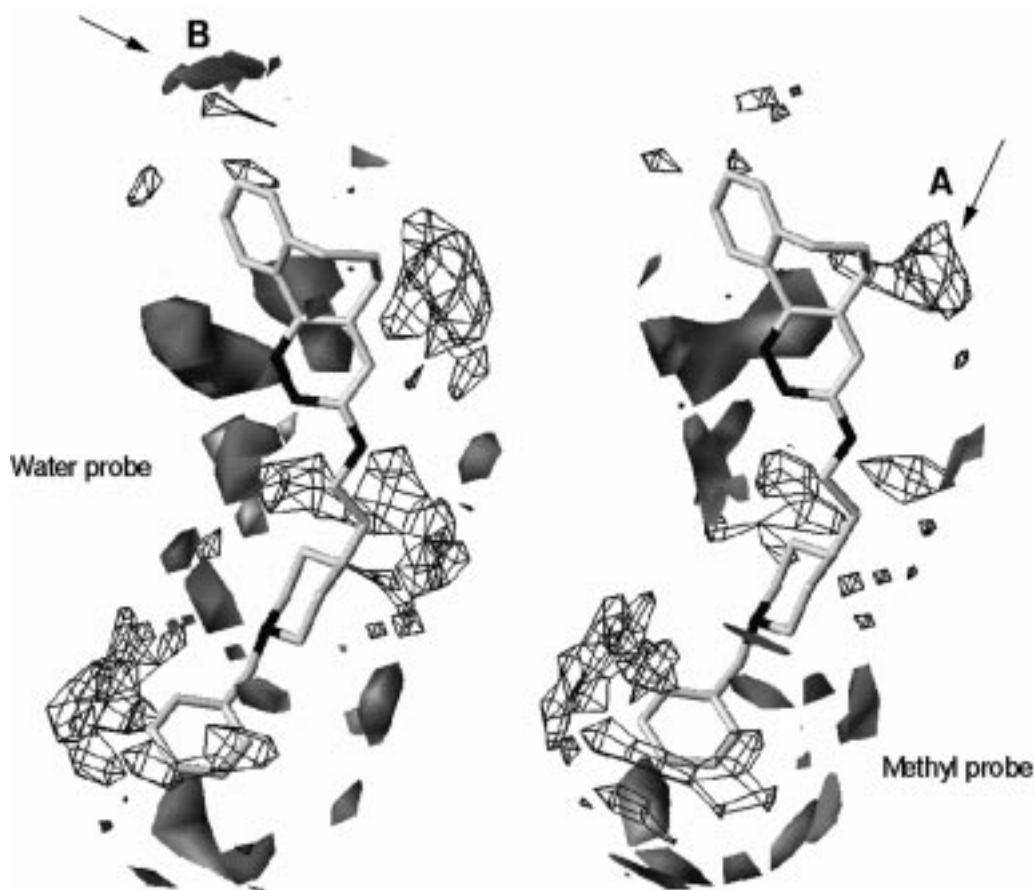


Figure 8. PLS coefficient maps obtained using the water probe (left side) and the methyl probe (right side). Opaque fields are contoured at -0.003 , grid fields are contoured at $+0.003$.

[48]. The crystal structure of the AChE complexed with the benzylpiperidine derivative, donepezil, has been made available. Like donepezil, our most potent inhibitors contain a benzylpiperidine moiety which shows a similar position and orientation when compared with the published crystal structure. Both kind of inhibitors adopt a comparable conformation in the narrow binding pocket (Figure 9). The indanone ring of donepezil stacks against the indole ring of Trp279, in the peripheral binding site, by a classical π - π interaction. A similar interaction was found for the arylpyridazine part of our inhibitors. In the reported X-ray structure, donepezil makes no direct hydrogen bond to an amino acid residue of the binding pocket. Only water-bridged hydrogen bonds have been detected for donepezil, as proposed for the described aminopyridazine compounds.

Conclusions

The study was initially undertaken to explore the binding of the developed aminopyridazine compounds to AChE. The availability of crystal structures of AChE separately complexed with four structurally diverse inhibitors enabled us to establish and analyze a model of the binding site. Using GRID interaction fields and molecular mechanics methodology we were able to dock the inhibitors into the model and so assess and refine the model. The good match of predicted and experimental structures gave confidence that such a strategy provides important information for the drug design process. Using a combination of receptor-based alignment and 3D QSAR yielded a significant and predictive model, indicated by the high cross-correlation coefficients and the low SDEP values. The model has proven to be successful both as a generator of design ideas and for the prediction of biological activities.

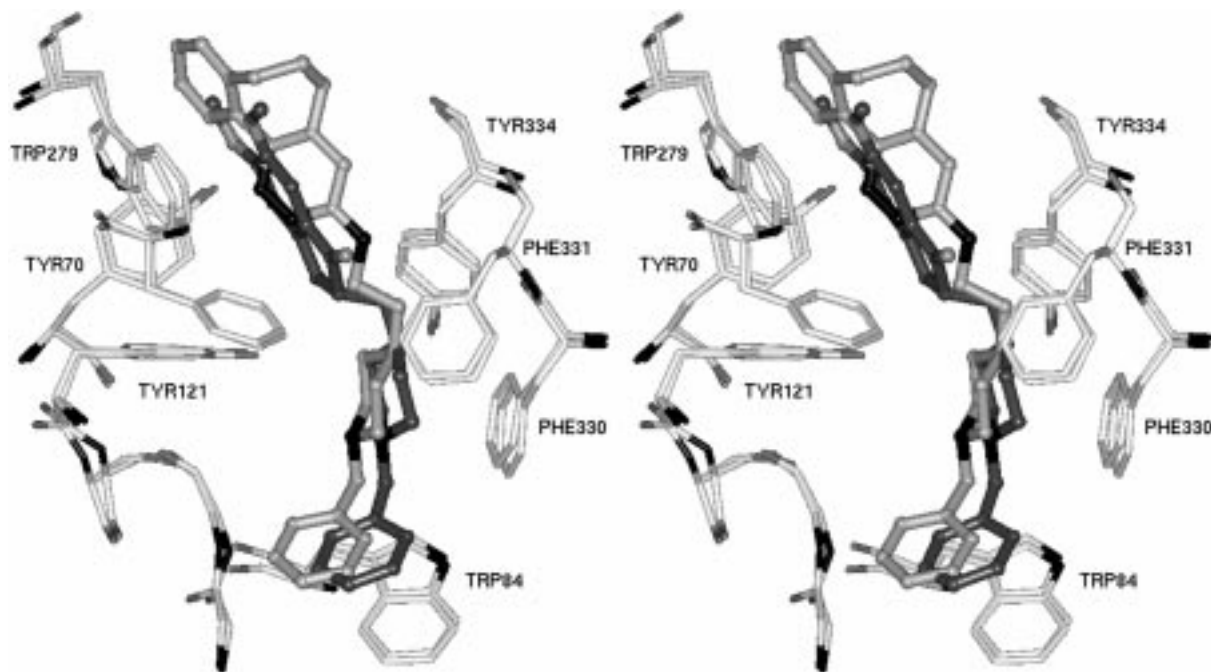


Figure 9. Stereo view of the experimentally determined AChE-donepezil complex and the predicted AChE-aminopyridazine complex. The aminopyridazine inhibitor **4j** (light-gray) adopts a similar conformation as donepezil (dark-gray) in the corresponding complex.

The availability of the crystal structure of the structurally related inhibitor donepezil further confirmed the accuracy of our strategy in predicting the binding conformation of AChE inhibitors.

Acknowledgements

The authors wish to thank Professor S. Clementi and Dr G. Cruciani, University of Perugia, for providing the GOLPE software and Professor P. Goodford for providing the GRID software.

References

- Kowall, N.W., *Alzheimer Disease and Associated Disorders*, 13 (1999) 11.
- Fine, R.E., *Alzheimer Disease and Associated Disorders*, 13 (1999) 82.
- Davies, P. and Maloney, A., *Lancet*, 2 (1976) 1403.
- Terry, R.D., Masliah, E. and Salmon, D.P., *Ann. Neurol.*, 30 (1991) 572.
- Giacobini, E., *Jpn J. Pharmacol.*, 74 (1997) 225.
- Wagstaff, A.J. and McTavish, D., *Drugs Aging*, 4 (1994) 510.
- Bryson, H.M. and Benfield, P., *Drugs Aging*, 10 (1997) 234.
- Fulton, B. and Benfield, P., *Drugs Aging*, 9 (1996) 60.
- Enz, A., Boddeke, H., Gray, J. and Spiegel, R., *Ann. N.Y. Acad. Sci.*, 640 (1991) 272.
- Inestrosa, N.C., Alvarez, A., Perez, C.A., Moreno, R.D., Vicente, M., Linker, C., Casanueva, O., I.; Soto, C. and Garrido, A., *Neuron*, 16 (1996) 881.
- Giacobini, E.; Mori, F. and Lai, C.C., *Ann. N.Y. Acad. Sci.*, 777 (1996) 393.
- Taylor, P. and Lappi, S., *Biochemistry*, 14 (1975) 1989.
- Schalk, I., Ehret-Sabatier, L., Bouet, F., Goeldner, M. and Hirth, C., *Eur. J. Biochem.*, 219 (1994) 155.
- Contreras, J.M., Parrot, I., Sippl, W., Rival, Y.M. and Wermuth, C.G., *J. Med. Chem.* (2000) submitted.
- Wermuth, C.G. and Exinger, A., *Agressologie*, 13 (1972) 285.
- Sussman, J.L. and Silman, I., *Science*, 253 (1991) 872.
- Harel, M. and Sussman, J.L., *Proc. Natl. Acad. Sci. USA*, 90 (1993) 9031.
- Raves, M.L., Harel, M., Pang, Y.P., Silman, I., Kozikowski, A.P. and Sussman, J.L., *Nat. Struct. Biol.*, 4 (1997) 57.
- Tame, J.R.H., *J. Comput. Aid. Mol. Des.*, 13 (1999) 99.
- Böhm, H.J., *J. Comput. Aid. Mol. Des.*, 12 (1998) 309.
- Böhm, H.J., *J. Comput. Aid. Mol. Des.*, 8 (1994) 243.
- Wang, R., Liu, L., Lai, L. and Tang, Y., *J. Mol. Model.*, 4 (1998) 379.
- Ha, S., Andreani, R., Robbins, A. and Muegge, I., *J. Comput. Aid. Mol. Des.*, 14 (2000) 435.
- Waller, C.L., Oprea, T.I., Giolitti, A. and Marshall, G.R., *J. Med. Chem.*, 36 (1993) 4152.
- Ortiz, A.R., Pastor, M., Palomer, A., Cruciani, G., Gago, F. and Wade, R.C., *J. Med. Chem.*, 40 (1997) 1136.
- Cho, S.J., Garsia, M.L., Bier, J. and Tropsha, A., *J. Med. Chem.*, 39 (1996) 5064.
- Vaz, R.J., McLean, L.R. and Pelton, J.T., *J. Comput. Aid. Mol. Des.*, 12 (1998) 99.
- Sippl, W., *J. Comput. Aid. Mol. Des.*, 14 (2000) 559.

29. Contreras, J.M., Rival, Y., Chayer, S., Bourguignon, J.J. and Wermuth, C.G., *J. Med. Chem.*, 42 (1999) 730.
30. Ellman, G.L., Courtney, K.D., Andres, V., Featherstone, J. and Featherstone, R.M. *Biochem. Pharmacol.*, 7 (1961) 88.
31. Allen, F.H., Kennard, O. and Watson, D.G., *Struct. Correl.*, 1 (1994) 71.
32. Weiner, S.J., Kollman, P.A., Case, D.A., Singh, U.C., Ghio, C., Alagona, G., Profeta, S. and Weiner, P.J., *J. Am. Chem. Soc.* 106 (1984) 765.
33. Weiner, S.J., Kollman, P.A., Nguyen, D.T. and Case, D.A., *J. Comput. Chem.*, 13 (1986) 230.
34. Singh, U.C. and Kollman, P.A., *J. Comput. Chem.*, 5 (1984) 129.
35. Madura, J.D., Briggs, J.M., Wade, R.C., Davis, M.E., Luty, B.A., Ilin, A., Antosiewicz, J., Gilson, M.K., Bagheri, B., Scott, L.T. and McCammon, J.A., *Comput. Phys. Commun.*, 91 (1995) 57.
36. Goodford, P.J., *J. Med. Chem.*, 28 (1985) 849.
37. Morris, G.M., Goodsell, D.S., Huey, R. and Olson, A.J., *J. Comput. Aid. Mol. Des.*, 8, (1994) 243.
38. Goodsell, D.S., Morris G.M. and Olson, A.J., *J. Mol. Recognit.*, 9 (1996) 1.
39. Rao, M.J. and Olson, A.J., *Prot. Struct. Funct. Gen.*, 34 (1999) 173.
40. PrGen 1.5.6, Biographics Laboratory, Basel, Switzerland.
41. Vedani, A. and Dunitz, J.D., *J. Am. Chem. Soc.*, 107 (1985) 7653.
42. Vedani, A. and Huhta, D.W., *J. Am. Chem. Soc.*, 112 (1990) 269.
43. GOLPE version 4.0, Multivariate Infometric Analysis, Perugia, Italy.
44. Baroni, M., Constantino, G., Cruciani, G., Riganelli, D., Valigli, R. and Clementi, S., *Quant. Struct.-Act. Relat.*, 12 (1993) 9.
45. Cruciani, G. and Watson, K., *J. Med. Chem.*, 37 (1994) 2589.
46. Pastor, M., Cruciani, G. and Clementi, S., *J. Med. Chem.* 40 (1997) 1455.
47. Oprea, T.I. and Garcia, A.E., *J. Comput. Aid. Mol. Des.*, 10 (1996) 186.
48. Kryger, G., Silman, I. and Sussman, J.L., *Structure Fold. Des.* 15 (1999) 297.